Available online at www.sciencedirect.com
SCIENCE DIRECT®
Thin Solid Films 453–454 (2004) 182–186
thin solid films
www.elsevier.com/locate/tsf

Microstructures and film properties of $La_{0.7}Ca_{0.3}CoO_3$ produced by pulsed reactive crossed-beam laser ablation

M.J. Montenegro[a], M. Döbeli[b], T. Lippert[a,*], S. Müller[c], A. Weidenkaff[d], P.R. Willmott[a,e], A. Wokaun[a]

[a]*Paul Scherrer Institut, CH-5232 Villigen PSI, Switzerland*
[b]*Paul Scherrer Institut c/o ETH Hönggerberg, CH-8093 Zurich, Switzerland*
[c]*Euresearch, Effingerstr. 19, CH-3001 Bern, Switzerland*
[d]*University of Augsburg, Universitätstr. 1, D-86159 Augsburg, Germany*
[e]*Physical Chemistry Institute, University of Zürich, Winterthurerstr. 190, 8057 Zurich, Switzerland*

Abstract

The quality and microstructure of $La_{0.7}Ca_{0.3}CoO_3$ films produced by pulsed reactive crossed-beam laser ablation are analyzed considering composition, crystallographic orientation and morphology. The effects of cooling conditions, deposition with an oxygen background and of an additional N_2O gas pulse are studied. The analysis indicates that the best film quality is obtained for films deposited in the presence of the gas pulse and the oxygen background, followed by a fast cooling. The presence of the different oxidizing sources influences the crystallographic orientation of the grown films.

Keywords: Pulsed reactive crossed-beam laser ablation; Perovskite; Morphology

1. Introduction

Perovskite type oxides (ABO_3) are promising candidates as catalysts for solid oxide fuel cells [1] and metal–air batteries [2]. The large variety of A and B ions that can fit in the crystallographic structure gives a rise to a high diversity of reactions where perovskites can potentially be used as catalysts [3]. In particular, lanthanum cobaltates have been considered as low cost substitutes for noble metals in oxygen electrodes [4]. The application of $La_{1-x}Ca_xCoO_3$ (LCCO) as a bifunctional catalyst, i.e. catalyst for oxygen reduction and evolution for metal/air batteries, was advanced for rechargeable zinc/air batteries by Müller et al. [5]. To study and compare the catalytic activity of different perovskite phases, it is necessary to prepare electrodes on inactive substrates with well-defined electrolyte/oxide interfaces to exclude the influence of the binder and/or the support material (e.g. carbon). Pulsed reactive crossed-beam laser ablation (PRCLA) has been described in detail [6], and successfully applied to the growth of LCCO films [7], producing the correct oxygen stoichiometry in the films without any additional processing step, i.e. annealing in an oxygen atmosphere.

The main objective of this experimental study is to analyze in detail the different deposition parameters, which result in the best quality film, i.e. stoichiometry, crystallography and morphology. The 'best' films will be used as a model system for studying the electrochemical properties of different perovskites for both oxygen reactions (oxygen reduction and evolution).

2. Experimental

$La_{0.7}Ca_{0.3}CoO_3$ films were deposited on MgO(1 0 0) at 650 °C, using a KrF excimer laser ($\lambda = 248$ nm, 17 ns pulse length, 21 000 pulses), with a laser fluence of 7.6 J/cm^2 and a repetition rate of 10 Hz. The target material a $La_{0.7}Ca_{0.3}CoO_3$ rod was located 4.5 cm from the substrate. Two oxidizing sources were used during the experiments: a synchronized N_2O pulse (99.999% purity, pulse length of 400 μs, backing pressure = 2 bar, chamber pressure 5×10^{-6} mbar) and oxygen from a leak valve to provide an additional background pressure of $\approx 8\times10^{-4}$ mbar during the deposition. The time

*Corresponding author. Tel.: +41-56-3104076; fax: +41-56-3102485.
E-mail address: thomas.lippert@psi.ch (T. Lippert).

0040-6090/04/$ - see front matter © 2003 Elsevier B.V. All rights reserved.
doi:10.1016/j.tsf.2003.11.102

Table 1
Stoichiometry of the LCCO films deposited under different conditions

Film name	Deposition condition	Stoichiometry
A	Gas pulse (2 bar)	$La_{0.68}Ca_{0.32}Co_{0.93}O_{2.75}$
B	Oxygen background (8×10^{-4} mbar)	$La_{0.6}Ca_{0.4}Co_{0.98}O_{2.5}$
C	Gas pulse (2 bar) + oxygen back	$La_{0.68}Ca_{0.32}Co_{0.91}O_{2.91}$
1	Slow cooling	$La_{0.69}Ca_{0.31}Co_{0.94}O_{2.5}$
2	Fast stepwise cooling	$La_{0.7}Ca_{0.3}Co_{0.95}O_{2.76}$
3	Fast cooling	$La_{0.68}Ca_{0.32}Co_{0.91}O_{2.9}$

delay between the gas pulse and the laser pulse was 400 μs, for which the maximum interaction between the ablation plasma and the gas pulse is achieved, details are described elsewhere [8].

The influence of the oxidizing source was investigated in a first set of experiments in which films were produced, using (i) the gas pulse only (A), (ii) applying an oxygen background (B) and (iii) with both oxidizing sources present (C). As a post-treatment the films were cooled with the fast procedure (see below).

In a second set of experiments, the influence of the cooling procedure was studied. Three films deposited using both oxidizing sources were cooled with three different procedures: a slow cooling using a ramp with a rate of 5 °C/min (1); a faster stepwise cooling, where an initial rapid cooling step (≈175 °C in 1 min) is followed by a stepwise reduction over 50 min, which resembles a half-parabolic change in temperature (2); and a fast cooling, where the chamber was vented after the deposition and the films were removed after 15 min (≈40 °C/min) (3).

The film thickness and surface roughness were determined with a profilometer (Dektak 8000). The crystalline structure and texture of the films have been studied by X-ray diffraction measurements in Bragg–Brentano geometry using Cu Kα radiation. The film stoichiometry was determined by Rutherford backscattering spectroscopy (RBS) measurements using a 2 MeV ^{4}He beam and a surface barrier silicon detector. The collected data were analyzed using the RUMP program [9]. The morphology of the films was measured with atomic force microscopy in contact mode.

3. Results and discussion

The interaction of the gas pulse with the ablation plume results in an emission that is much brighter and extends further from the target, as compared to that obtained with an 8×10^{-4} mbar O_2 background alone. Films grown with the O_2 background and/or gas pulse are dark and mirror-like, independent of the cooling conditions. The film thickness, measured by the profilometer, can be controlled by the number of laser pulses during the deposition. In general, 21 000 pulses result in a thickness of approximately 200 nm with a roughness in the range of 2–4 nm. The film stoichiometry measured by RBS has an error of 5%. No nitrogen incorporation was observed in the grown films.

3.1. Effect of the different gases used during film deposition

The compositions of the deposited films are presented in Table 1. The stoichiometry changes with the different deposition conditions. When the films are grown only in the presence of 8×10^{-4} mbar of oxygen background, lower amounts of La, Ca and oxygen are observed, while the best oxygen stoichiometry is obtained when the film is deposited using the gas pulse and the oxygen background. The presence of only one oxidizing source always produces films with lower oxygen content, in agreement with the pressure and the oxidizing nature of the gas used. The effect of different gases during the formation of multicomponent metal-oxides has been investigated for a long time [10,11]. The oxygen requirements during growth of oxides are controlled by the oxidation kinetics and the thermodynamic phase stability at the growth temperature [10]. When pulsed laser deposition (PLD) is used as a film growing technique, a large amount of material is deposited in a very short time separated by periods with no vapor flux. This makes it necessary to have a high flux of oxygen available to oxidize the species that arrived at the substrate. In principle, the oxygen could originate exclusively from the oxide target, without the necessity of an additional oxidizing source. However, only a fraction of the oxygen is released as atoms (neutrals and ions), the remaining is O_2 [12]. The adsorption probability of O_2 will be less than unity due to the inefficient adsorption at the surface [13] compared to the high sticking probability of atomic O. The fact that the oxygen molecules have a lower probability of remaining at the substrate surface makes it necessary to utilize an additional oxidizing source for the effective oxidation of the cations during the film growth.

The flux of oxygen molecules is much lower in the case of the 8×10^{-4} mbar background, as compared to the flux of liberated target atoms created by laser ablation. The kinetic requirement for stoichiometric oxide growth is therefore not fulfilled (to produce an

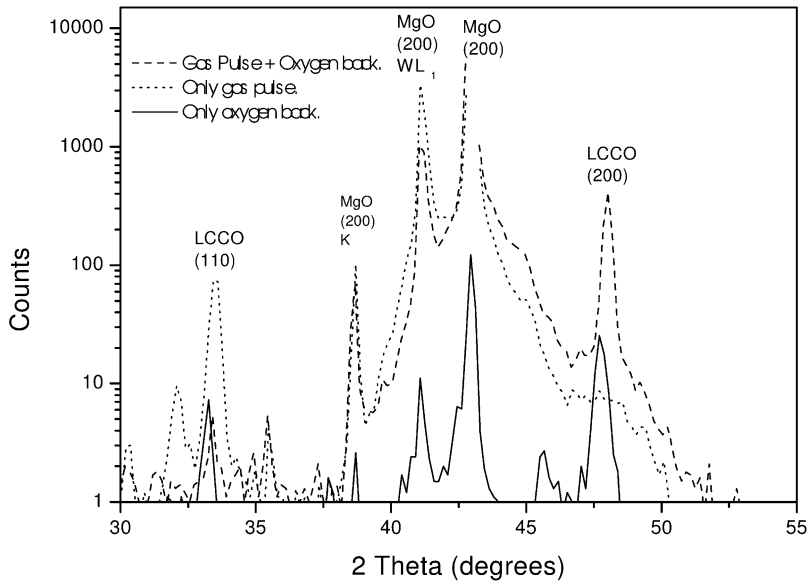

Fig. 1. XRD spectra of $La_{0.7}Ca_{0.3}CoO_3$ deposited with different oxidizing sources.

effective oxidation of the cationic species), resulting in films with an oxygen deficiency. With the synchronized N_2O gas pulse, an excess of oxygen atoms (originating from the dissociation of N_2O by collisional fragmentation by photons from the plasma or electron-impact [11]) is created, and the species from the LCCO target arrive simultaneously at the substrate, resulting in films with better oxygen stoichiometry. The films with the best oxygen stoichiometry are obtained when both oxidizing sources are applied. To understand these results we have to consider not only the arrival time of the particles at the substrate, but also the time between each pulse. There exists an oxygen diffusion equilibrium that influences the oxygen content of the growing film [14,15]. This equilibrium is shifted to loss of oxygen from the film, when only the background is present (8×10^{-4} mbar of oxygen). In the case of the N_2O pulse only, there is enough oxygen present to obtain the stoichiometry during the arrival of the atoms at the substrate but the low background of 2×10^{-6} mbar between the pulses will shift the diffusion equilibrium even further in the direction of 'out diffusion', with the influence of the gas pulse being more important. When both the N_2O pulse and the additional oxygen background are applied, large amount of atomic oxygen will arrive together with the species originated from the target. There is now more oxygen available between the pulses, which minimize the loss of the volatile oxygen from the surface. Therefore, the films with the highest oxygen stoichiometry are obtained.

Fig. 1 shows the XRD pattern of LCCO films grown with different oxidizing sources. In all cases only the formation of a crystalline LCCO phase is observed, but the orientation depends on the oxidizing source. An intense LCCO(2 0 0) peak at 47.97° and a weak LCCO(1 1 0) reflection at 33.18° are observed for those films which were deposited using the gas pulse and the oxygen background. Those films deposited only with oxygen background, two peaks (2 0 0) and (1 1 0) with nearly equal intensity are observed, whereas films deposited using the gas pulse only reveal nearly an exclusive orientation in the (1 1 0) plane. This data strongly suggest that the phase structure and preferential orientation, i.e. from (2 0 0) to (1 1 0), depends on the applied oxidizing source. The origin of this behaviour is not clear and will be the subject of further studies.

The morphology of the films grown under the different conditions is shown in Fig. 2. The film deposited with the oxygen background (Fig. 2A) presents a combination between large (25 nm) and small columns (5.7 nm), where each column is formed by a single grain. The roughness obtained from the AFM images is in agreement with the values obtained by the profilometer ($\approx$7 nm). The 2D figure reveals a quite dense structure with almost no holes. The AFM image of the film deposited with the N_2O gas pulse (Fig. 2B) presents a very dense microstructure, with smaller grains than for the films growth with the O_2 background. An average grain size of $\approx$17 nm and a roughness of $\approx$6 nm are observed. Fig. 2C shows the AFM images of a film deposited using both oxidizing sources. The 2D picture appears similar to that in Fig. 2A, but with larger lateral features. The average size of the features is $\approx$40 nm with a roughness of $\approx$11 nm.

The morphology of PLD films has been extensively studied as a function of the pressure of the background gas [16]. Many structural features can be explained by the 'microstructure zones model' of Thornton [17].

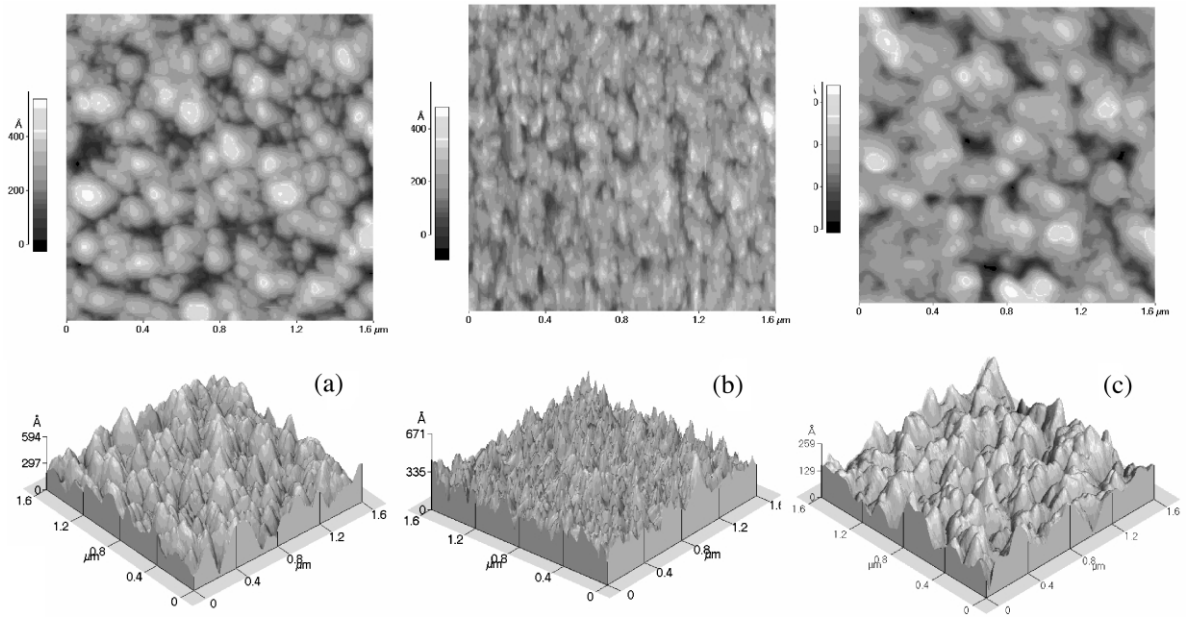

Fig. 2. AFM images of the LCCO films: (A) deposited in an oxygen background 8×10^{-4} mbar; (B) deposited without oxygen background using the N_2O pulse at 2 bar; (C) deposited with oxygen background and gas pulse.

Films grown with PRCLA are expected to reveal a different behaviour as the growth conditions are different to those applied in traditional PLD, where the O_2 background is normally in the range of 10^{-2} mbar. Other parameters that have to be considered are the transfer of internal and kinetic energy from the ablated species to the gas pulse molecules. These collisions take place in the interaction region, close to the target surface. Due to the low background pressure the plasma expands rapidly and nearly becomes collision-free [18]. These initial collisions reduce the velocity of the expanding plasma particles significantly. Furthermore, collisions result in scattering of the plasma cloud, causing the particles to arrive at the substrate with a broader angular distance. The arriving particles are partially thermalized before reaching the film surface and inducing a 'self shadowing' effect [11] which produces films with a fine vertical fibrous microstructure called 'zone I columnar porous morphology' in Thornton's model. When employing only the oxygen background, the pressure is so small that almost no scattering occurs in the plasma and the particles retain their energy. The resulting film becomes less porous and the grain size increases. The dense film presents a bimodal distribution of large grains surrounded by small ones in a region, called zone T. When both the gas pulse and the oxygen background are applied, the microstructure is similar to zone T but with a more random distribution probably due to the pronounced scattering in the plume.

3.2. Effect of the cooling condition

No pronounced differences in the heavy atom content of the films are observed, when different cooling procedures are applied, while the oxygen stoichiometry varies clearly (Table 1). The oxygen stoichiometry must depend on the cooling rate, considering that the cooling procedure is performed in the absence of oxygen to obtain a better crystallographic quality [7]. The chamber is kept in vacuum, i.e. at 4×10^{-6} mbar, during the cooling procedure 1 and 2, suggesting that oxygen diffusion (significant at temperatures above 300 °C) occurs. In the case of the cooling procedure 3, i.e. fast cooling, the cooling is performed at atmospheric pressure where the amount of oxygen is high enough to shift this diffusion equilibrium and thereby avoid losses of oxygen from the film.

The XRD pattern of those films cooled under vacuum (shown in Fig. 3) reveal the presence of LCCO(1 1 0) and LCCO(2 0 0). The film cooled at atmospheric pressure shows a preferential orientation in the (2 0 0) plane and only a small (1 1 0) reflection is observed. This indicates that the best crystallographic quality is produced by the fast cooling procedure.

The morphology of these films was analyzed and all of them present a zone T microstructure according to Thornton's model. The feature size indicates that the cooling velocity influence the average particle height. Slowly cooled films present an average particle height distribution of approximately 17 nm, while the fast

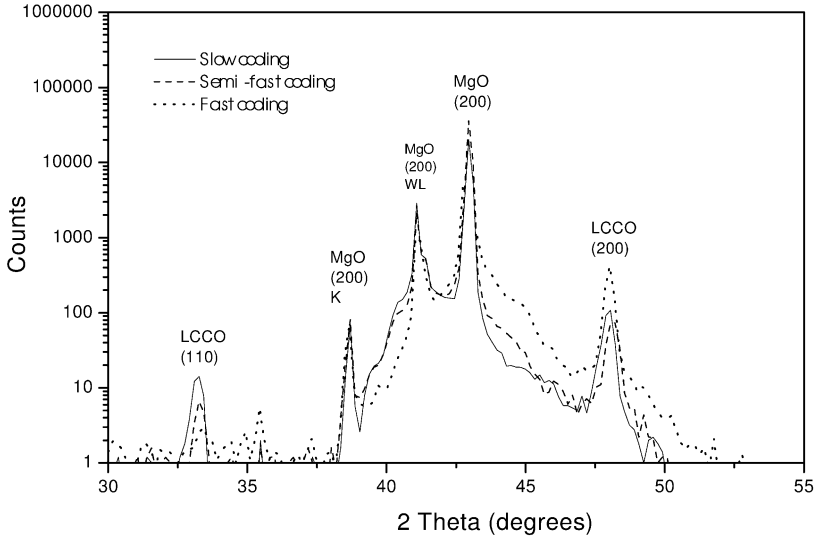

Fig. 3. XRD spectra of $La_{0.7}Ca_{0.3}CoO_3$ cooled with different procedures.

stepwise cooled films have a distribution of approximately 20 nm and the fast cooled films a distribution of 40 nm. These variations may be explained by the different cooling rates, i.e. slow cooling results in longer time scales for a possible surface arrangement of clusters while with shorter time scales the final morphology will resemble the appearance of the films directly after deposition.

4. Conclusions

The oxygen stoichiometry of LCCO films changes depending on the applied oxidizing source and the cooling velocity. An oxygen deficient structure is formed when the films are cooled slowly or produced just with the oxygen background. No deficiency is detected when the films are fast cooled and both oxidizing sources are applied. The crystallographic orientation can be controlled with the deposition parameters and cooling procedure. Single oriented films are obtained when both oxygen sources and fast cooling procedure are applied. The particle height and type of morphology can be influenced by varying the oxidizing source and the cooling procedure after film deposition. In general, the best quality films (i.e. oxygen stoichiometry and crystallographic orientation) are obtained by using the N_2O pulse with the O_2 background followed by a fast cooling procedure at atmospheric pressure.

References

[1] J.T. Cheung, P.E.D. Morgan, D.H. Lowndes, X.Y. Zheng, J. Breen, Appl. Phys. Lett. 62 (1993) 2045.
[2] S. Müller, F. Holzer, O. Haas, J. Appl. Electrochem. 28 (1998) 895.
[3] J. Alonso, M.J. Martinez-Lope, H. Falcon, R.E. Carbonio, Phys. Chem. Chem. Phys. 1 (1999) 3025.
[4] R.N. Singh, B. Lal, Indian J. Chem., Part A 40 (2001) 1037.
[5] S. Müller, O. Haas, C. Schlatter, C. Comninellis, J. Appl. Electrochem. 28 (1998) 305.
[6] P.R. Willmott, Appl. Phys. A 69 (1999) 437.
[7] M.J. Montenegro, M. Döbeli, T. Lippert, S. Müller, B. Schnyder, A. Weidenkaff, P.R. Willmott, A. Wokaun, Phys. Chem. Chem. Phys. 4 (2002) 2799.
[8] P.R. Willmott, J.R. Huber, Rev. Mod. Phys. 72 (2000) 1.
[9] L.R. Doolittle, Nucl. Instrum. Methods B 15 (1986) 227.
[10] A. Gupta, B.W. Hussey, Appl. Phys. Lett. 58 (1991) 1211.
[11] A. Gupta, B.W. Hussey, M.Y. Chern, Physica C 200 (1992) 263.
[12] C.H. Chen, R.C. Phillips, M.P. McCann, Phys. Rev. B 39 (1989) 2744.
[13] J.R. Engstrom, T. Engel, Phys. Rev. B 41 (1990) 1038.
[14] M. Cherry, M.S. Islam, C.R.A. Catlow, J. Solid State Chem. 118 (1995) 125.
[15] Y.L. Yang, A.J. Jacobson, C.L. Chen, G.P. Luo, K.D. Ross, C.W. Chu, Appl. Phys. Lett. 79 (2001) 776.
[16] M. Koubaa, A.M. Haghiri-Gosnet, R. Desfeux, Ph. Lecoeur, W. Prellier, B. Mercey, Appl. Phys. Lett 93 (2003) 5227.
[17] J.A. Thornton, J. Vac. Sci. Technol. A 4 (1986) 3059.
[18] M.J. Montenegro, C. Clerc, T. Lippert, S. Müller, A. Weidenkaff, P.R. Willmott, A. Wokaun, Appl. Surf. Sci. 208–209 (2003) 46.